

## RAIN, SUN AND SHADING EFFECTS ON THE THERMODYNAMICS OF SOILS

### Gerson H. dos Santos

Pontifical Catholic University of Paraná – PUCPR/CCET  
Thermal Systems Laboratory  
Rua Imaculada Conceição, 1155 - Curitiba – PR – 80215-901 – Brazil  
gerson.santos@pucpr.br

### Nathan Mendes

Pontifical Catholic University of Paraná – PUCPR/CCET  
nathan.mendes@pucpr.br

### Roberto Zanetti Freire

Pontifical Catholic University of Paraná – PUCPR/CCET  
roberto.freire@pucpr.br

**Abstract.** *This paper presents the software Solum that has been developed to model the coupled heat and moisture transfer in porous soils. It has been conceived to be a fast simulation tool using a robust solver for the strongly-coupled problem of heat and mass transfer through an unsaturated porous soil. The Solum models predict temperature and moisture content profiles within soils under different sort of boundary conditions for both diffusion and capillary regimes of moisture migration, which can be easily read by building simulation codes in order to provide important information on ground heat transfer and moisture capacity. The present version allows executing 3-D heat and moisture transfer simulation so that it shows the effects of temperature and moisture in the soils. A new module was also added into this version, making possible simulations with different boundary conditions at the upper soil surface. This model allows simulating combined effects of sun and shade or rain.*

**Keywords:** *simulation tool, ground heat transfer, hygrothermal simulation of soils.*

## 1. Introduction

For understanding physical, chemical and biological phenomena in soils, information of temperature and moisture content is indispensable. For example, in the area of building hygrothermal analysis, most simulation programs do not consider the moisture transport through the building envelope, mainly through ground. Among several difficulties found in the ground heat flow calculation, some shall be cited: the multidimensional phenomenon; the transient behavior of the soil and the great number of involved parameters in the coupled heat and mass transfer.

In the building, the presence of moisture within the envelope and ground implies an additional mechanism of transport: absorbing or releasing latent heat of vaporization. In this way, the Solum program has been conceived to model the coupled three-dimensional heat and moisture transfer in soils, based on the theory of Philip and De Vries (1957), which is one of the most disseminated and accepted mathematical formulation for studying heat and moisture transfer through porous soils, considering both vapor diffusion and capillary migration.

The Solum linearized set of equations was obtained by using the finite-volume method and the MTDMA-MultiTriDiagonal Matrix Algorithm (Mendes et al., 2002). In this way, the software has been conceived to be numerically robust with a fast simulation code.

Some building physics studies involving the conduction heat transfer through the ground can be found in the literature. The first experimental study concluded that the heat loss through the ground is proportional to the size of its perimeter. However, Bahnfleth (1989) observed that the area and shape must be taken into account as well.

Hagentoft (1996) presented general formulae by which the heat loss and the temperature in the ground can be determined for the case of infinite ground water flow rate.

Janssen et al. (2002) elaborated an analysis of heat loss through a basement and presented as false a generally accepted postulate in building simulation: the combined heat and mass transfer in ground can be ignored for the heat flow calculation through the building foundation.

Among many works found in the literature in soils, we should cite some such as Brink and Hoogendoorn (1983). In their work, groundwater losses due to conduction and natural convection heat transfer modes were analyzed and verified that convection losses are mainly dependent on soil permeability. In the same way, Krarti (1996) discussed the effect of spacial variation of soil thermal properties on slab-on-ground heat transfer by using the Interzone Temperature Profile Estimation (ITPE) technique.

Brasil et al. (2003) presented an analytical and experimental methodology to determine the ground temperature under a translucent plastic cover, used to dry grains.

Freitas and Prata (1996) elaborated a numerical methodology for thermal performance analysis of power cables under the presence of moisture migration in the surrounding soil. They utilized a two-dimension finite-volume approach to solve the governing equations and the boundary conditions did not take any phase-change effect into account.

Despite inaccuracies related to building energy calculation, the effects of humidity can also generate other problems in buildings such as mold growth (Lucas et al., 2002; Moon and Augenbroe, 2003).

In order to demonstrate the effects of the coupled 3-D heat and moisture transfer of the ground in the building simulation, a new module was added into this version, making possible simulations with different boundary conditions at the upper soil surface. This model allows simulating combined effects of sun and shade or rain.

In this analysis a sandy silt soil was considered and the TRY (Test Reference Year) weather data for Brasilia-Brazil was utilized, showing the importance of considering in building envelope analysis the 3-D heat and moisture transfer in soils.

## 2. Nomenclature

$c_m$  - mean specific heat (J/kg K)

$D_{Tl}$  - liquid phase transport coefficient associated to a temperature gradient (m<sup>2</sup>/s K)

$D_{Tv}$  - vapor phase transport coefficient associated to a temperature gradient (m<sup>2</sup>/s K)

$D_{\theta l}$  - liquid phase transport coefficient associated to a moisture content gradient (m<sup>2</sup>/s)

$D_{\theta v}$  - vapor phase transport coefficient associated to a moisture content gradient (m<sup>2</sup>/s)

$D_T$  - mass transport coefficient associated to a temperature gradient (m<sup>2</sup>/s K)

$D_\theta$  - mass transport coefficient associated to a moisture content gradient (m<sup>2</sup>/s)

$h_m$  - mass convection coefficient (m/s)

$h$  - convection coefficient (W/m<sup>2</sup> K)

$j_v$  - vapor flow (kg/m<sup>2</sup>s)

$j$  - total flow (kg/m<sup>2</sup> s)

$L$  - latent heat of vaporization (J/kg)

$M$  - molecular mass (kg/kmol)

$P_s$  - saturated pressure (Pa)

$prev$  - previous iteration

$q_r$  - solar radiation (W/m<sup>2</sup>)

$\mathfrak{R}$  - universal gas constant (J/kmol K)

$R_{ol}$  - long-wave radiation (W/m<sup>2</sup>)

$T$  - temperature (°C)

$t$  - time (s)

$\alpha$  - solar absorptivity

$\varepsilon$  - emissivity

$\phi$  - relative humidity

$\lambda$  - thermal conductivity (W/m<sup>2</sup> K)

$\rho_0$  - solid matrix density (kg/m<sup>3</sup>)

$\rho_l$  - water density (kg/m<sup>3</sup>)

$\rho_{v,\infty}$  - vapor density in the surrounding air far from the soil surface (kg/m<sup>3</sup>)

$\rho_{v,y=H}$  - vapor density at the upper surface of the soil domain (kg/m<sup>3</sup>)

$\theta$  - volume basis moisture content (m<sup>3</sup>/m<sup>3</sup>)

## 3. Mathematical Model

The governing equations, based on the theory of Philip and De Vries (1957), to model heat and mass transfer through porous media, are given by Eqs. (1) and (2). The energy conservation equation is written in the form

$$\rho_0 c_m (T, \theta) \frac{\partial T}{\partial t} = \nabla \cdot (\lambda (T, \theta) \nabla T) - L(T) (\nabla \cdot \mathbf{j}_v) \quad (1)$$

and the mass conservation equation as

$$\frac{\partial \theta}{\partial t} = -\nabla \cdot \left( \frac{\mathbf{j}}{\rho_l} \right), \quad (2)$$

where  $\rho_0$  is the solid matrix density ( $\text{m}^3/\text{kg}$ ),  $c_m$ , the mean specific heat ( $\text{J/kg K}$ ),  $T$ , temperature ( $^\circ\text{C}$ ),  $t$ , time (s),  $\lambda$ , thermal conductivity ( $\text{W/m K}$ ),  $L$ , latent heat of vaporization ( $\text{J/kg}$ ),  $\theta$ , volumetric moisture content ( $\text{m}^3/\text{m}^3$ ),  $j_v$ , vapor flow ( $\text{kg/m}^2 \text{K}$ ),  $j$ , total flow ( $\text{kg/m}^2 \text{K}$ ) and  $\rho_l$  the water density ( $\text{kg/m}^3$ ).

The total flow ( $\mathbf{j}$ ) is given by summing the vapor flow ( $\mathbf{j}_v$ ) and the liquid flow ( $\mathbf{j}_l$ ). The vapor flow can be described as

$$\frac{\mathbf{j}}{\rho_l} = - \left( D_T(T, \theta) \frac{\partial T}{\partial x} + D_\theta(T, \theta) \frac{\partial \theta}{\partial x} \right) \mathbf{i} - \left( D_T(T, \theta) \frac{\partial T}{\partial y} + D_\theta(T, \theta) \frac{\partial \theta}{\partial y} \right) \mathbf{j} - \left( D_T(T, \theta) \frac{\partial T}{\partial z} + D_\theta(T, \theta) \frac{\partial \theta}{\partial z} + \frac{\partial K_g}{\partial z} \right) \mathbf{k} \quad (3)$$

with  $D_T = D_{Tl} + D_{Tv}$  and  $D_\theta = D_{\theta l} + D_{\theta v}$ , where  $D_{Tl}$  is the liquid phase transport coefficient associated to a temperature gradient ( $\text{m}^2/\text{s K}$ ),  $D_{Tv}$  is the vapor phase transport coefficient associated to a temperature gradient ( $\text{m}^2/\text{s K}$ ),  $D_{\theta l}$ , liquid phase transport coefficient associated to a moisture content gradient ( $\text{m}^2/\text{s}$ ),  $D_{\theta v}$ , vapor phase transport coefficient associated to a moisture content gradient ( $\text{m}^2/\text{s}$ ),  $D_T$ , mass transport coefficient associated to a temperature gradient ( $\text{m}^2/\text{s K}$ ) and  $D_\theta$ , mass transport coefficient associated to a moisture content gradient ( $\text{m}^2/\text{s}$ ).

The upper surface of the physical domain (Fig.1) is exposed to short and long-wave radiations, convection heat transfer and phase change as boundary conditions.

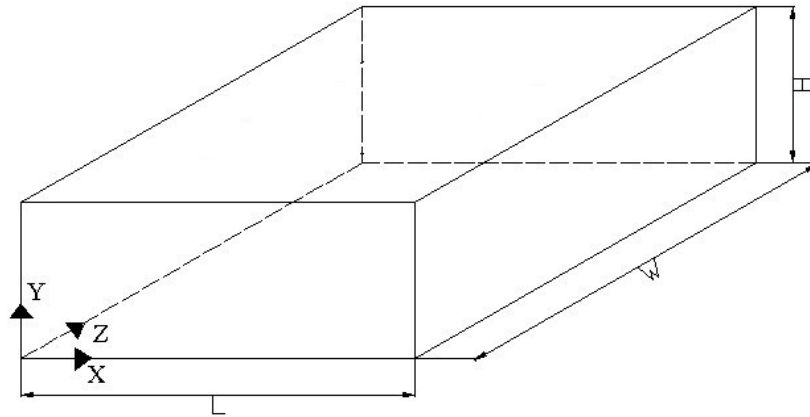


Figure 1. Physical domain of soil

This way, for  $Y=H$ , the energy balance becomes

$$\left( \lambda(T, \theta) \frac{\partial T}{\partial y} \right)_{y=H} + (L(T) j_v)_{y=H} = h(T_\infty - T_{y=H}) + \alpha q_r + L(T) h_m (\rho_{v,\infty} - \rho_{v,y=H}) - \varepsilon R_{ol}, \quad (4)$$

where  $h(T_\infty - T_{y=H})$  represents the heat exchanged by convection with the external air, described by the surface conductance  $h$ ,  $\alpha q_r$  is the absorbed short-wave radiation and  $L(T) h_m (\rho_{v,\infty} - \rho_{v,y=H})$ , the phase change energy term. The loss from long-wave radiation is defined as  $R_{ol}$  ( $\text{W/m}^2$ ),  $\varepsilon$ , the surface emissivity. The solar absorptivity is represented by  $\alpha$  and the mass convection coefficient by  $h_m$ , which is related to  $h$  by the Lewis' relation.

Similarly, the mass balance is written as

$$\left( D_{\theta}(T, \theta) \frac{\partial \theta}{\partial y} + D_T(T, \theta) \frac{\partial T}{\partial y} \right)_{y=H} = \frac{h_m}{\rho_l} (\rho_{v,\infty} - \rho_{y=H}). \quad (5)$$

The others surfaces were all considered adiabatic and impermeable as well.

Equations 4 and 5 show a vapor concentration difference,  $\Delta \rho_v$ , on their right-hand side. This difference is between the porous surface and air and is normally determined by using the values of previous iterations for temperature and moisture content, generating additional instability. Due to the numerical instability created by this source term, the solution of the linear set of discretized equations normally requires the use of very small time steps, which can be exceedingly time consuming especially in long-term soil simulations; in some research cases, a time period of several decades is simulated, taking into account the tridimensional transfer of heat and moisture transfer through a very refined grid.

In order to increase that simulation time step, Mendes et al. (2002) presented a procedure to calculate the vapor flow, independently of previous values of temperature and moisture content. In this way, the term ( $\Delta \rho_v$ ) was linearized as a linear combination of temperature and moisture content, viz.,

$$(\rho_{v,\infty} - \rho_v(s)) = C_1 (T_{\infty} - T(s)) + C_2 (\theta_{\infty} - \theta(s)) + C_3 \quad (6)$$

where

$$\begin{aligned} C_1 &= A \frac{M}{\mathfrak{R}} \phi, \\ C_2 &= \frac{M}{\mathfrak{R}} \left( \frac{P_s(s)}{T(s)} \right)^{prev} \left( \frac{\partial \phi}{\partial \theta(s)} \right)^{prev}, \\ C_3 &= \frac{M}{\mathfrak{R}} \left[ \left( \frac{P_s(s)}{T(s)} \right)^{prev} R(\theta^{prev}(s)) + \phi_{\infty} (R(T_{\infty}) - R(T^{prev}(s))) \right], \end{aligned}$$

where

$R$  is a residual function of  $\left( \frac{P_s}{T} \right)$ ,  $P_s$ , saturated pressure (Pa),  $\mathfrak{R}$ , universal gas constant (J/kmol K),  $M$ , molecular mass (kg/kmol),  $\phi$ , relative humidity,  $prev$ , previous iteration and  $A$  is the straight-line coefficient from the approximation  $\left( \frac{P_s}{T} \right) = AT + B$ .

#### 4. Simulation Procedure

In order to analyze the boundary conditions effects, the governing equations were solved using the finite- volume methodology (Patankar, 1980). The differential equations were integrated in each control volume and a fully-implicit scheme was adopted for the time derivatives. The robustly algorithm MTDMA (MultiTridiagonal-Matrix Algorithm) was used to solve the 3-D problem in porous soils (Mendes et al., 2002). In this study, the soil was considered sandy silt type (properties taken from Oliveira et al., 1993).

A physical domain of 15.5m x 5m x 15.5m and a uniform mesh constituted by 9610 nodes (31 x 10 x 31) was utilized. In this version of the computational code, the upper surface of the soil is divided in 9 domains (Fig. 2) and different boundary conditions can be used in order to illustrate the importance of the multidimensional aspects of ground heat transfer.

The region 5 (Fig. 2) was considered with constant values of temperature and relative humidity of 24°C and 50 % with a constant convection heat transfer coefficient of 3 W/m²K, representing, in this way, a conditioned building space. The other regions were submitted to the TRY (Test Reference Year) weather data for the city of Brasília-Brazil (South latitude of -15.87°), with a constant convection heat transfer coefficient of 10 W/m²K and a constant long-wave radiation loss of 100 W/m² and emissivity of 0.3.

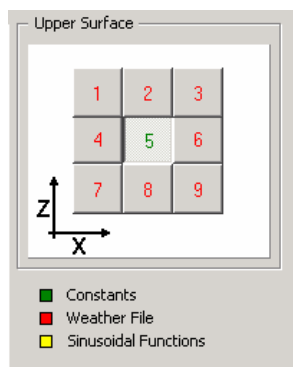


Figure 2. Upper surface domain.

The regions 7, 8 and 9 were considered shaded during all the time. On the other hand, the regions 1, 2, 3, 4 and 6 were submitted to solar radiation (absorptivity = 0.3) except when solar radiation is totally ignored for comparison purposes, illustrating sun effects. To analyze the effect of rain, the superficial nodes of these regions were saturated from March 1<sup>st</sup> to October 31<sup>st</sup> and the solar radiation was ignored in this case. In all cases, the other surfaces of the soil were considered adiabatic and impermeable. In the simulation, a warm-up period of 2 years was employed with a time step of 1 hour.

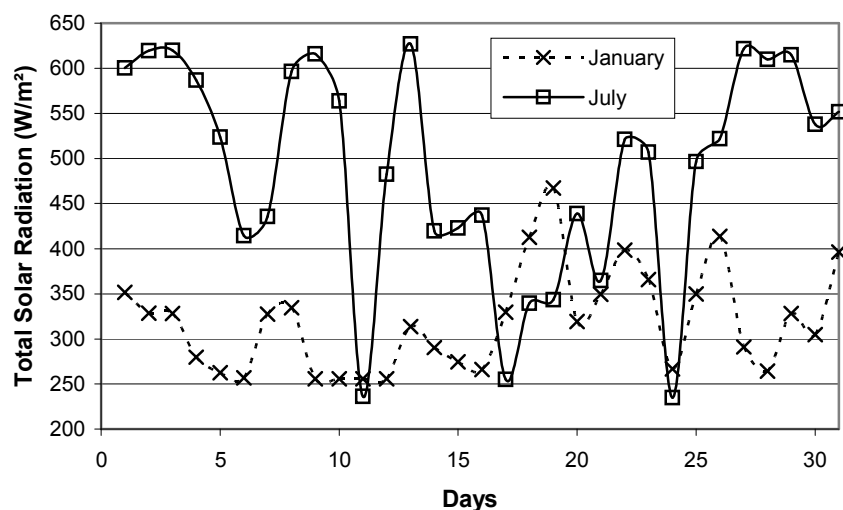


Figure 3. Daily-averaged values of total solar radiation for Brasilia in January and July.

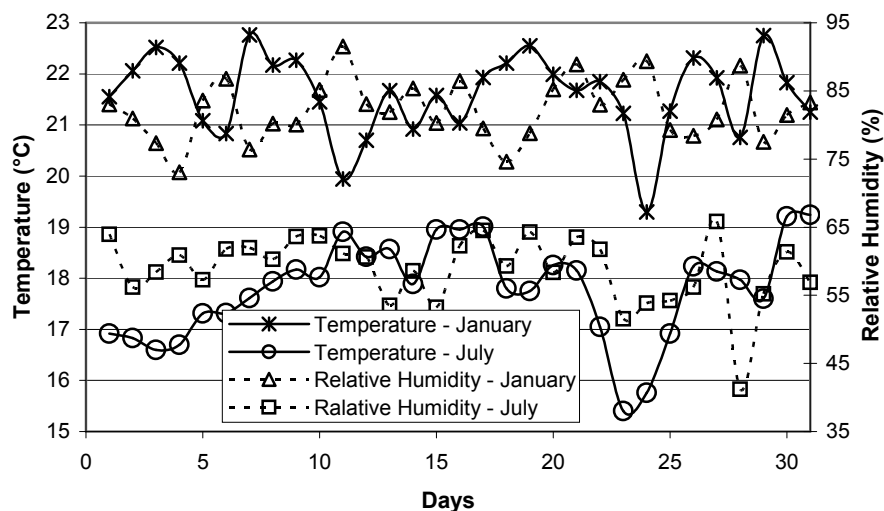


Figure 4. Daily-averaged values of temperature and relative humidity for Brasilia in January and July.

Figures 3 and 4 show the daily-averaged values of total solar radiation, temperature and relative humidity in January and July months from TRY (Test Reference Year) weather data for the city of Brasília-Brazil.

## 5. Results

In Fig. 5, we notice that the soil temperature under the conditioned space, after a warm-up period of two years, nearly reaches the air temperature of 24 °C; except for the case when there is no short-wave radiation around the conditioned space. This can be explained by the fact the tangential temperature gradients are low, especially when solar radiation is not included as a boundary condition.

As the city of Brasília (Lat. =  $-15.87^\circ$ ) is very dry in the winter (July), higher evaporation rates occur at this time of the year, decreasing slightly the surface temperature even when solar radiation is present. In Fig. 5.e, we can also observe a higher heat penetration when solar radiation is considered with low temperature gradients.

Figure 5 depicts as well the importance of considering the multidimensional aspects of the combined heat and moisture transfer through unsaturated porous soils. On the other hand, we believe that shallower soil domains, e. g., lower than 2m, could be considered when the analysis is focused on the hygrothermal performance of building envelopes. It is also shown in Fig. 5 that the rain boundary condition is not appropriated for the analysis of temperature profiles within the ground as the energy balance is barely modified in an indirect way. However, that boundary condition is adequate to quantify the rain influence on the moisture content profile as illustrated in Fig. 6.

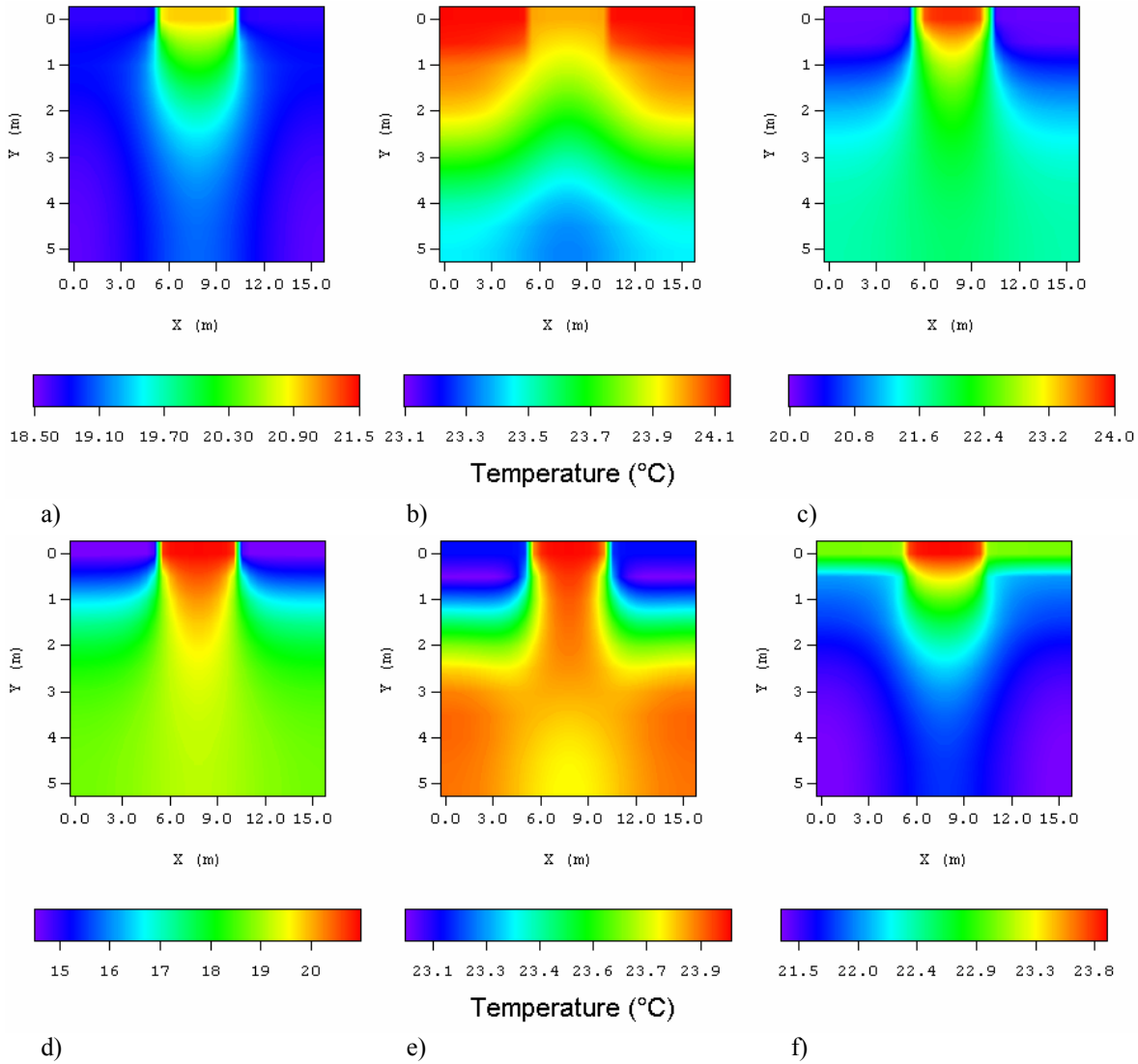


Figure 5. Average temperature distributions through a X-Y section for the months of January and July. a) Without solar radiation in January; b) With solar radiation in January; c) With rain in January; d) Without solar radiation in July; e) With solar radiation in July; f) With rain in July.

Figure 6 clearly shows dryer soils when solar radiation is considered, as the surface temperatures (Figs. 5.b and 5.e) go up, promoting higher evaporation rate that dries out the soil as a whole, especially in July when the relative humidity is low (Fig. 6.e).

Figure 6.c presents a high moisture content at the upper surface in contact with external air due to the “rainy” boundary condition, which was assumed only from March to October in the two pre-simulation years. We can notice from the month of January to July, that some of the rain water ( $\approx 9\%$ ) has been accumulated at a depth around 0.7 m, while the surface is dryer due to the evaporation occurred since the month of January. In this way, the high hygric soil capacity can be remarkably observed.

In Fig. 6, we notice, for three cases in the month of January, that the moisture content at the surface in contact with the conditioned space is nearly the same. However, in July, it is noted a higher moisture content in the case of no solar radiation than the one found for the “rainy” case. This can be explained due to the higher evaporation rates occurred after the rainy period under the presence of Sun.

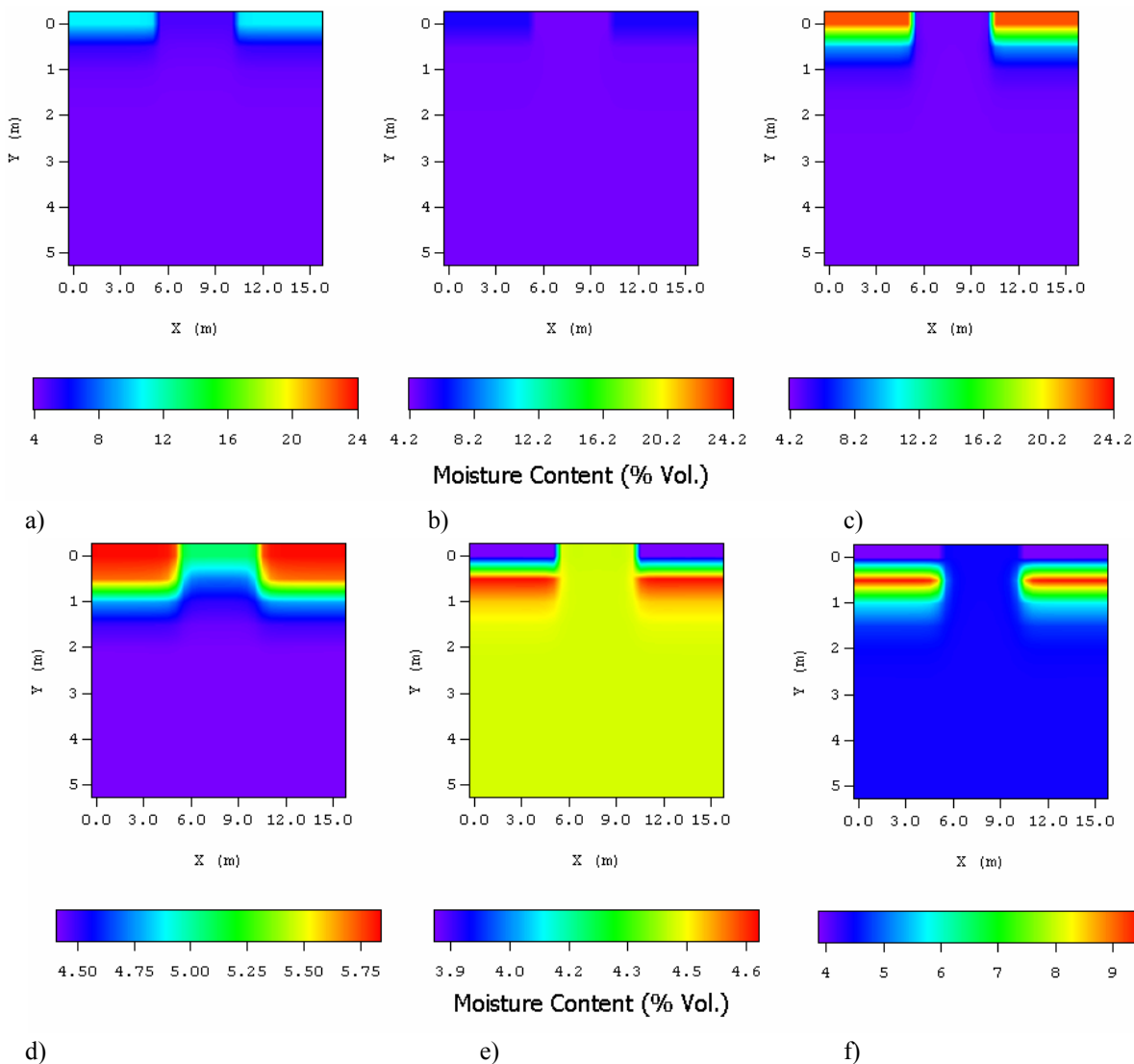


Figure 6. Moisture content distribution through a X-Y section for the months of January and July. a) Without solar radiation on January; b) With solar radiation on January; c) With rain on January; d) Without solar radiation on July; e) With solar radiation on July; f) With rain on July.

## 6. Conclusions

We have presented the Solum 1.5 program for predicting temperature and moisture content 3-D spatial distributions. Generated text files can be easily read by building simulation codes, providing their models with temperature and moisture content distributions for any given time. This information can be used to analyse the use of soils for passive cooling/heating by coupling it to building simulation programs such as Domus (2003), in geothermal heat pump models and in the integration of the building with buried-duct ventilation systems.

It has also been noticed the multidimensional aspects of ground heat transfer for building simulation tools. On the other hand, shallower depths can be considered as the temperature and moisture content gradients are low in deep soil sections, which makes whole-building hygrothermal simulation coupled with soil simulation less time consuming.

For further work, we recommend the improvement of the rain model in both energy and mass balances and the integration of the presented model with a whole-building simulation code.

## 7. References

- Bahnfleth W. P., 1989, "Three-dimensional modelling of slab-on-grade heat transfer", Building Simulation Conference – IBPSA 89, 133-138.
- Brasil, S. B., Ferreira, A. G., Valle, R. M., Cortez, M. F. B., Andrade, R. M., 2003, "A Methodology to Determine the Temperature Distribution on the Ground Under a Plastic Cover Exposed to the Solar Radiation.", 17<sup>th</sup> International Congress of Mechanical Engineering – COBEM.
- Brink, G. J. Van Den, Hoogendoorn, C. J., 1983, "Ground Water Flow Heat Losses for Seasonal Heat Storage in the Soil.", Solar Energy, Vol. 30, N°4, pp. 362-371.
- Freitas, D. S., Prata, A.T., 1996, "Thermal Performance of Underground Power Cables with Constant and Cyclic Currents in Presence of Moisture Migration in the Surrounding Soil.", IEEE Transactions on Power Delivery, Vol. 11, No 3.
- Hagentoft, C., 1996, "Heat Losses and Temperature in the Ground under a Building with and without Ground Water Flow--I. Infinite Ground Water Flow Rate", *Building and Environment*, Vol. 31, No. 1, pp.3-11.
- Janssen, H., Carmeliet, J., Hens, H., 2002, "The influence of soil moisture in the unsaturated zone on the heat loss from building via the ground.", *Journal of Thermal Envelope and Building Science*, Vol. 25, No 4, pp. 275-298.
- Krarti, M., 1996, "Effect of Spatial Variation of Soil Thermal Properties on Slab-on-Ground Heat Transfer.", *Building and Environment*, Vol. 31, No. 1, pp. 51-57.
- Lucas, F., Adelard, L., Garde, F., Boyer, H., 2002, "Study of moisture in buildings for Hot Humid Climates." *Energy and Building*, Vol. 34, pp. 345-355.
- Mendes, N., Philippi, P. C., Lamberts, R., 2002, "A new Mathematical Method to Solve Highly Coupled Equations of Heat and Mass Transfer in Porous Media.", *International Journal of Heat and Mass Transfer*, Vol. 45, p. 509-518.
- Mendes, N., Oliveira, R. C. L. F., Santos, G.H., 2003, "Domus 2.0: A Whole-Building Hygrothermal Simulation Program." *Building Simulation 2003, Eighth International IBPSA Conference. International Building Performance Simulation Association*, Eindhoven, Netherlands, Vol. 2, pp. 863-870.
- Moon, H. J., Augenbroe, G., 2003, "Evaluation of hygrothermal models for mold growth avoidance prediction." *Eighth International IBPSA Conference. International Building Performance Simulation Association*, Eindhoven, Netherlands, Vol. 2, pp. 895-901.
- Oliveira, A. A. J; Freitas, D. S., 1993, "Influência do Meio nas Difusividades do Modelo de Phillip e Vries." *Relatório de Pesquisa*, UFSC.
- Patankar S.V. , 1980, "Numerical Heat Transfer and Fluid Flow."
- Philip, J. R., D. A. de Vries., 1957, "Moisture Movement in Porous Media under Temperature Gradients." *Trans Am geophysical Union*, Vol. 38, pp. 222-232.

## 8. Responsibility notice

The authors are the only responsible for the printed material included in this paper.